Dynamic characterisation of railway track superstructure for the analysis of ground borne vibration in soft subsoil

Maryam Hallaj[1*], *Li* Wang[1], *Stefano* Muraro[1], *Zili* Li[1], and *Cristina* Jommi[1,2]

[1] Department of Civil Engineering and Geosciences, Delft University of Technology, Delft, The Netherlands
[2] Department of Civil and Environmental Engineering, Politecnico di Milano, Milano, Italy

Abstract. The railway track superstructure including rails, sleepers and ballast is the primary interface between the train induced dynamic loads and the underlying embankment and subsoil, and plays a crucial role in load transfer, energy dissipation, and vibration attenuation. Accurate assessment of the train induced dynamic response of soft soils requires prior characterisation of the load transferred by the track superstructure. Hammer impact testing is an effective method for evaluating track dynamics, as it excites a broad frequency range and enables identification of the system natural frequencies through resonance amplification in the measured response. This study analyses the dynamic response of a laboratory railway track model consisting of rails, sleepers, and ballast subjected to hammer impact excitation as an aid to the development of a reliable finite element (FE) model of railways on soft soils. A three-dimensional finite element model of the experimental setup is developed in LS-DYNA to simulate the transient dynamic response of the track system. The numerical results are compared with the vibration time history and the frequency response function measured experimentally on the ballast layer. The finite element model is used to perform a sensitivity analysis to evaluate the influence of relevant input parameters of the track on the dynamic response measured on the ballast layer. The results suggest that different track components govern distinct frequency ranges of the system response, enabling efficient modelling strategies for railway systems on soft soils.

1 Introduction

A substantial proportion of the railway network in the Netherlands is founded on soft subsoil deposits such as peat and clay. These ground conditions present significant geotechnical challenges for railway infrastructure, including excessive deformation, differential settlement, and amplified vibration levels under repeated train loading [1, 2]. Increasing passenger and freight demand has intensified the need to enhance network capacity through higher axle loads, increased train speeds, and more frequent traffic operations. To maintain acceptable serviceability, safety, and long-term performance under these evolving operational requirements, it is essential to improve understanding of the dynamic interaction between the train, track, embankment, and underlying soft subsoil.

The train-track-embankment-subsoil interaction can be investigated using experimental, analytical [3], and numerical approaches, each offering distinct advantages and limitations. Experimental studies remain essential because they provide direct measurements of system response and enable calibration and validation of predictive models. Experimental investigations are classified into three categories: field measurements, element-scale testing, and physical model testing.

The primary advantage of field measurements lies in their ability to capture the response of the railway system under true operational conditions and at full scale, providing valuable information including ground vibration, track deflection, settlement, pore water pressure generation, and stress changes during train passage [4, 5]. Field measurements are costly, location-specific, and the interpretation is influenced by uncertain or variable boundary conditions, heterogeneous soil stratigraphy, environmental effects, and operational variability. Consequently, repeatability and controlled parametric investigation are limited.

On the other hand, element-scale laboratory testing, such as cyclic triaxial, resonant column, or simple shear testing, is widely used to characterise soil behaviour under cyclic and dynamic loading [4, 6]. These tests provide essential information for constitutive model calibration, including stiffness degradation, damping, and strength characteristics. Nevertheless, they do not address the soil-structure interaction of railway systems, since track components, load transfer mechanisms, and system boundary effects are not explicitly included.

Physical models provide an intermediate and highly valuable approach by reproducing key aspects of the railway system under controlled laboratory conditions. Such tests allow investigating components interaction, load transfer mechanisms, and dynamic behaviour in a repeatable and cost-effective environment [7-10]. In this sense, physical modelling bridges the gap between element-scale material characterisation and full-scale

* Corresponding author: m.hallaj@tudelft.nl

field observations. Therefore, the experimental approaches should be regarded as complementary rather than independent methods.

Physical modelling is commonly combined with numerical simulations. A numerical model can be used efficiently to investigate the system behaviour, perform sensitivity studies, explore scenarios that are difficult to test experimentally, and support the design and the interpretation of the small scale model.

A reliable numerical simulation starts with a comprehensive model for the dynamic response of the track superstructure including the rails, sleepers, fasteners, and ballast. This system governs load distribution, vibration transmission, damping, and local resonance behaviour; therefore, it is a prerequisite for realistic prediction of railway induced ground response.

To this aim, this study leverages data from hammer impact excitation on a controlled laboratory physical test to set up a finite element model capable of reproducing those track components that prevail on the transmission of vibrations through the ballast towards the subsoil. Impact testing is an efficient modal identification technique because it excites multiple frequencies simultaneously, allowing the natural frequencies and resonance characteristics of the system to be determined from the measured response. The FE model is employed to perform a parametric investigation into the influence of key track component properties on the dynamic response of the railway track system. The FE model is intended to provide a reliable basis for subsequent modelling of railway systems incorporating embankment and soft subsoil layers.

2 Laboratory physical model

The experimental data are coming from laboratory hammer impact test performed at the Railway Engineering Section of TU Delft. The experimental programme was originally designed to investigate the influence of sensor installation methods on measured vibration characteristics of the ballast layer.

The physical modelling setup, shown in Fig. 1, consists of two rails supported by four sleepers resting on a ballast layer, 0.3 m thick, above a concrete slab base. During the experiment, hammer excitation is applied at the mid-span of the rail, while the vibration response is measured on the ballast surface between sleepers 2 and 3, indicated as the measurement point in Fig. 1. The dynamic response is recorded using both geophones and accelerometers to capture velocity and acceleration time histories, respectively.

Fig. 2 illustrates representative frequency domain responses obtained from the sensors. Differences between geophone and accelerometer measurements below 20 Hz are mainly attributed to sensor sensitivity and measurement characteristics within this frequency range. The results consistently identify four dominant resonance peaks between 20 and 120 Hz, corresponding to the dominant natural frequencies of the track system. The receptance amplitude gradually decreases with increasing frequency, indicating a reduction of the dynamic amplification at higher frequencies.

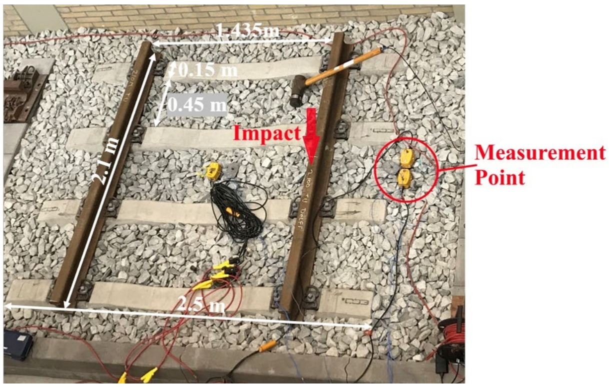

Fig. 1. Schematic of the testing setup.

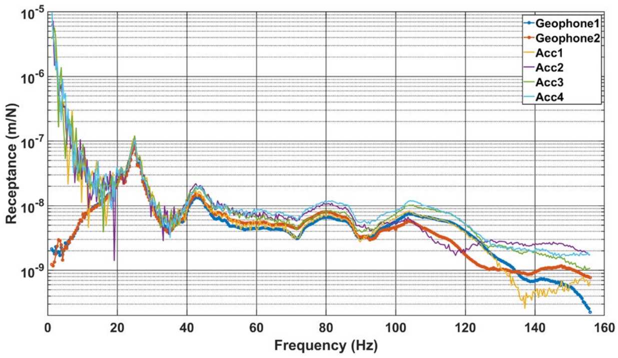

Fig. 2. Frequency domain response generated from the experimental measurements.

Despite the differences in installation methods, the measured responses show consistent resonance frequencies among the sensors. Therefore, only one representative geophone and one accelerometer response were selected for the sake of comparison between experimental data and results of the FE model.

3 Finite element model

3.1 Model geometry and discretisation

A 3D finite element (FE) model of the experimental setup was developed in LS-DYNA. The geometry of the FE model is constructed to reproduce the physical laboratory setup and is illustrated in Fig. 3.

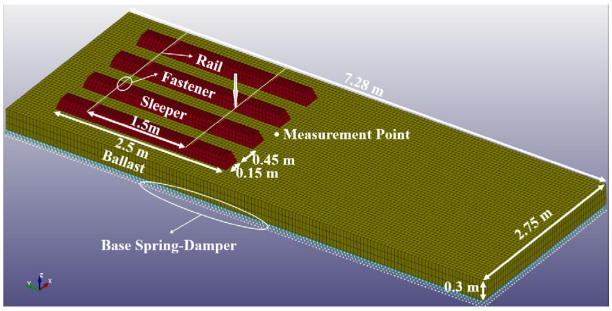

Fig. 3. Geometry of the FE model.

The rails are modelled as beams and discretised into 150 elements of 0.03 m length. The sleepers are modelled using 3000 3D solid hexahedral elements, with characteristic element sizes ranging from 0.03 m to 0.055 m. The ballast layer is modelled with 23100 hexahedral solid elements, with element sizes between 0.05 m and 0.1 m.

The fastener system is modelled using 6 discrete spring-damper elements per each rail seat. In total, 48 spring-damper elements are used through this part of the model. These elements are introduced to account for alleged vibration reduction and load transfer between rails and sleepers.

Force and vibration transfer between the sleepers and ballast layer is ensured through shared nodes at the sleeper-ballast interface. Beneath the ballast layer, 7896 pairs of distributed spring-damper elements are introduced to represent the equivalent stiffness and damping of the underlying support concrete structure.

3.2 Material properties

The material properties used in the reference FE model are summarised in Table 1. The rails and sleepers are modelled as linear elastic steel and concrete, respectively. The ballast layer is also modelled as a linear elastic material, as the focus of this study is on small-strain wave propagation. Damping is introduced on the ballast layer using the stiffness proportional damping at the element level implemented in LS DYNA [11], to primarily attenuate frequencies above 100 Hz. The damping coefficient used for the ballast layer is reported in Table1.

The fastener and base supports are modelled using discrete linear elastic springs and viscous damper elements. The parameters adopted in the reference simulation were taken from the literature [12-15].

Table 1. Material properties adopted in the reference simulation.

	Density $\rho[\mathrm{kg/m^3}]$	Elastic modulus $E[\mathrm{N/m^2}]$	Poisson ratio $\nu[-]$	Stiffness $k[\mathrm{N/m}]$	Damping D
Rail	7800	2.1E11	0.3	-	-
Sleeper	2400	2.2E10	0.3	-	-
Ballast	1800	1.3E8	0.3	-	0.25 [-]
Fastener	-	-	-	3.3E6	5E3 [N.s/m]
Base	-	-	-	3E4	30 [N.s/m]

3.3 Numerical considerations

An explicit dynamic analysis is chosen, which is well suited for transient dynamic analyses involving short-duration impact loading. The equations of motion are integrated in time using the explicit central difference scheme, subject to the Courant Friedrichs Lewy (CFL) stability condition.

Automatic time step control is implemented in LS-DYNA by computing the critical time step satisfying CFL criterion for each part of the model, choosing the smallest one and adopting a scaling factor (typically 0.9) to improve the efficiency of the algorithm [16]. A fixed time step of 4.48E-6 s fulfilled this criterion in all the analyses. The duration of the applied impact pulse was 1.9E-3 s. The temporal resolution is sufficient to accurately represent the impact loading history and the resulting wave propagation response.

Reduced (1-point) integration is used for the three-dimensional 8-node hexahedral solid elements. Although reduced integration improves computational efficiency, it may introduce nonphysical zero-energy deformation modes, commonly referred to as hourglass modes. To control these numerical instabilities, a stiffness controlled hourglass stabilisation is adopted with an hourglass coefficient of 0.1. In this formulation, the hourglass deformation increment accumulated over successive time steps is used to calculate stabilising forces (LS-DYNA hourglass type 4) [16].

The frequency range that can be reliably represented by the numerical model is governed by the mesh resolution and the wave propagation characteristics of the materials. Considering the maximum ballast element size of 0.1 m and adopting a minimum requirement of 10 nodes per wavelength for accurate wave transmission, the minimum wavelength in the model is 1 m. Based on the ballast material properties, the shear wave velocity is 165 m/s. Consequently, the upper reliable frequency limit of the model is estimated to be 165 Hz. This frequency range is considered appropriate, as it encompasses the frequency content of ground borne vibrations in the field, typically bounded by 100 Hz.

3.4 Loading conditions (Impact loading)

In the FE model, the hammer impact is represented as a short-duration force applied at the corresponding rail mid-span location (Fig. 3). The load-time history is approximated by a triangular pulse shown in Fig. 4. This simplified representation captures the essential characteristics of the impulse loading while guaranteeing computational efficiency.

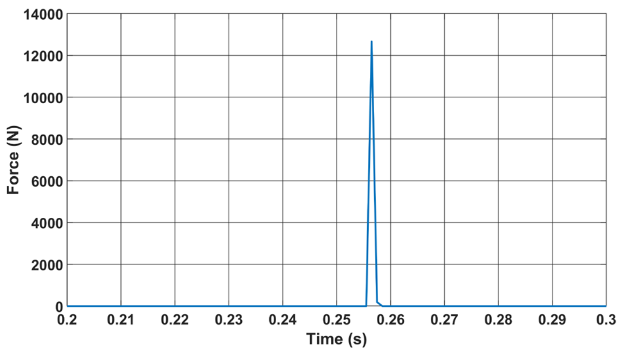

Fig. 4. Simulated hammer impact time history on the rail.

3.5 Boundary conditions

Appropriate boundary conditions are applied to replicate the laboratory support conditions. The lateral faces of the ballast layer are constrained in the horizontal and longitudinal directions, while vertical displacement is permitted. This allows vertical deformation while preventing unrealistic lateral spreading of the ballast, thereby approximating the confinement provided by the laboratory container.

At the base of the ballast layer, spring-damper supports are introduced to represent the dynamic stiffness and energy dissipation of the underlying support system. These elements simulate the influence of the omitted lower layers, including the laboratory foundation.

4 Results and analysis

4.1 Model assessment

The dynamic response of the measurement point located on the ballast layer is used for model assessment through comparison between numerical and experimental results in both the time domain (velocity and acceleration responses, Fig. 5a-b) and the frequency domain using the frequency response function (FRF) (Fig. 5c). In Fig. 5c, the receptance is calculated as displacement over force in the frequency domain.

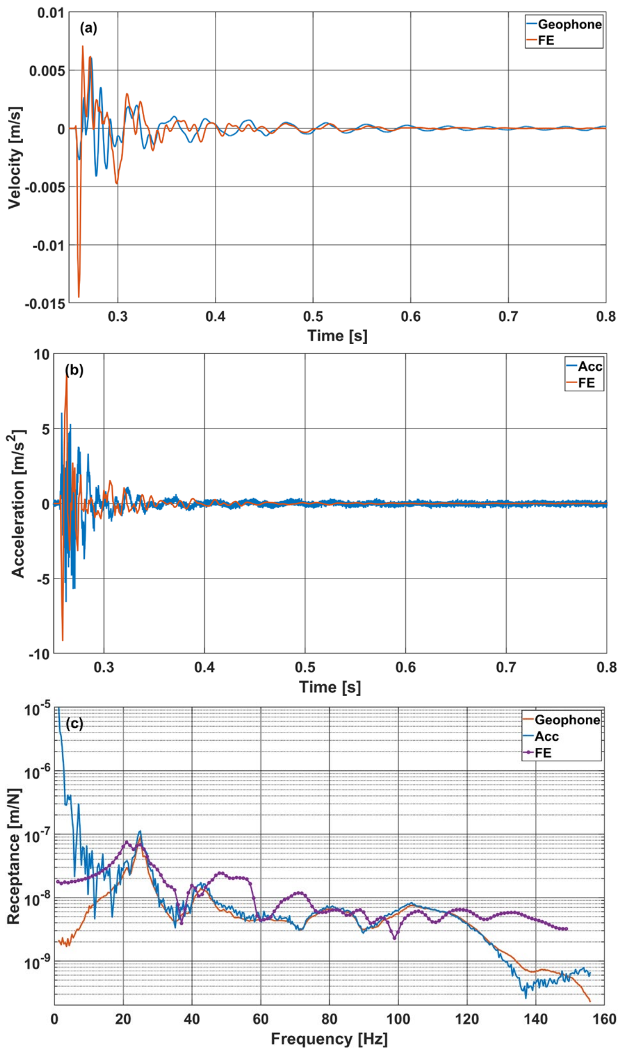

Fig. 5. Comparison between numerical and experimental results in terms of (a) velocity-time, (b) acceleration-time and (c) frequency domain.

Reasonable agreement is observed between numerical and experimental results in the time domain, considering that the material properties were taken from the literature.

The dominant peak vibration amplitudes are well captured by the model and the attenuation trend follows the experimental response. The time required for complete vibration decay is consistent in both cases, indicating that the damping characteristics of the system are represented in a realistic way.

In the frequency domain, the FRF obtained from the FE model shows good agreement with experimental measurements in the lower frequency range (<40 Hz). The system exhibits decay in energy content with increasing frequency, indicating that the dynamic response is dominated by frequency modes up to about 100 Hz. In this range, four resonance frequencies of the system are consistently visible in the numerical results. Above 100 Hz, the FE model exhibits additional nonphysical vibration modes and lower attenuation compared with the experimental response. It is worth noting that this frequency range is of limited practical interest when considering the effects of railway vibration propagation on the embankment stability, since high frequency vibration components are typically attenuated by radiation and material damping in the soil.

To further investigate vibration transmission through the track system, the FRFs at the rail and ballast layer are compared in Fig. 6, where the rail response is evaluated beneath the hammer impact location. Both responses show a gradual decrease in vibration energy with increasing frequency; however, the rail retains significantly higher energy over most of the investigated frequency range. This behaviour can be partly attributed to the modelling assumptions adopted in the present study, as no damping was assigned to the rail. Above approximately 50 Hz, the ballast response becomes strongly attenuated, while the rail continues to exhibit considerable vibration energy up to 150 Hz. This behaviour indicates that higher frequency vibrations are progressively attenuated by the system, whereas lower frequency components propagate more effectively toward the ballast and underlying support layers. A dominant resonance peak is observed around 20 Hz, corresponding to the first natural frequency of the coupled track system, while a smaller peak appears near 50 Hz in the rail response.

Overall, the model provides a reliable basis for subsequent parametric investigations of the system dynamic response.

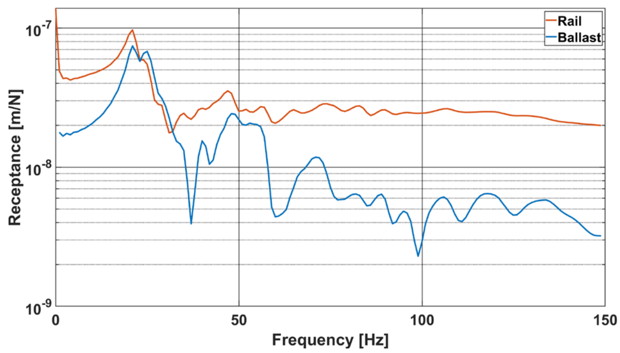

Fig. 6. Comparison of rail and ballast layer responses in terms of frequency domain response.

4.2 Parametric study setup

A parametric analysis was conducted to evaluate the influence of key parameters on the system response. The investigated parameters include:

- Fastener stiffness and damping
- Ballast stiffness and damping
- Base (foundation) stiffness and damping

The reference configuration for the parametric study corresponds to the FE model previously compared with the experimental measurements (Fig. 3). In each parametric analysis, only one parameter at a time was changed, while all other parameters were kept constant.

Three values are considered for each parameter (Table 2), covering the expected representative range of the system reported in the literature and field measurements for railway track systems [12-15]. The selected values represent low, intermediate, and high cases within the reported variation range. It should be noted that the discrete element parameters represent the stiffness and damping of individual connections; therefore, the value reported in the table is multiplied by 6 in the model. The effective fastener stiffness corresponds to six parallel spring elements per rail seat. In each of the results reported in the following sections, the blue line represents the reference case with the parameters in Table 1.

Table 2. Input values for the parametric analysis.

Parameters	Values		
Fastener stiffness [N/m]	3.3E6	2E7	3.8E7
Fastener damping [N.s/m]	5E2	5E3	1.25E4
Ballast Elastic modulus [Pa]	1.3E8	1.9E8	2.6E8
Ballast damping [-]	0.01	0.1	0.25
Base stiffness [N/m]	3E4	5E4	1.9E6
Base damping [N.s/m]	30	1E2	3E2

4.3 Influence of fastener properties

As shown in Fig. 7a, increasing the stiffness of the fastener has a limited influence on the overall attenuation trend of the time-domain response. In the frequency domain (Fig. 7b), the first dominant resonance peak remains largely unaffected, whereas a slight increase in response amplitude is observed on the higher modes. Above approximately 100 Hz, the FRF becomes smoother with reduced fluctuations as stiffness increases. This suggests that, provided the total stiffness of the fastener is at least equal 1.2 E8 N/m, it primarily influences the behaviour above 100 Hz.

Increasing fastener damping reduces vibration amplitudes across the entire time history (Fig. 8a), indicating more effective energy dissipation at the rail-sleeper interface. Higher damping also leads to faster attenuation of transient vibrations. In the case of low fastener damping, the high frequency components of the vibration are not effectively attenuated at the rail-sleeper interface. As a result, these high frequency components are transmitted directly to the ballast layer, leading to pronounced nonphysical high frequency oscillations in the time domain response.

At lower frequencies (<30 Hz), the first resonance peak remains largely unchanged (Fig. 8b). Damping results in a noticeable suppression of frequency content above 80 Hz in the ballast response. Therefore, fastener damping plays a key role in controlling higher frequency vibrations associated with rail-sleeper interaction, while having limited influence on the fundamental system modes.

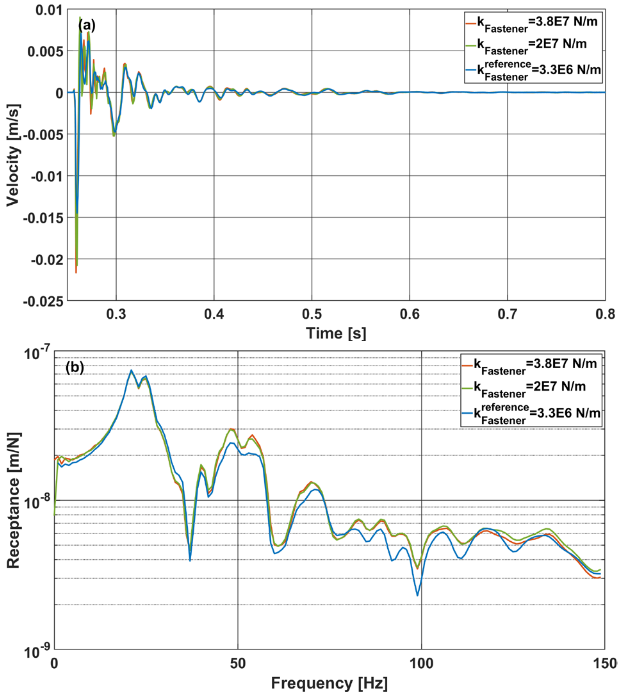

Fig. 7. Influence of fastener stiffness on the ballast vibration in terms of (a) time domain and (b) frequency domain.

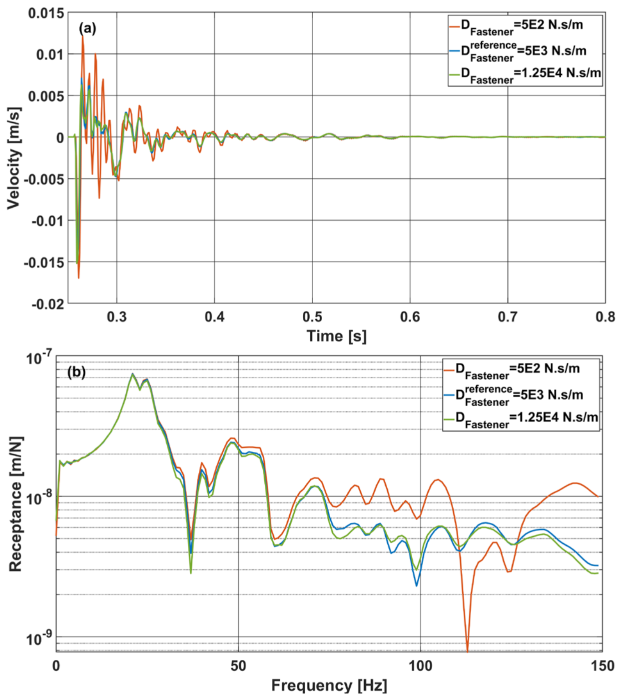

Fig. 8. Influence of fastener damping on the ballast vibration in terms of (a) time domain and (b) frequency domain.

4.4 Influence of ballast properties

4.4.1 Ballast stiffness (elastic modulus)

Increasing the elastic modulus of the ballast reduces the initial peak vibration amplitude due to increased support stiffness and reduced local deformation under impact loading (Fig. 9a). However, at later stages of the response, higher stiffness leads to more sustained vibration levels, indicating reduced strain energy dissipation. The lower ballast modulus exhibits slightly faster attenuation of vibrations, which can be attributed to increased energy dissipation during cyclic loading.

The FRF analysis (Fig. 9b) shows that increasing ballast stiffness results in a shift of the second and third resonance peaks toward higher frequencies, confirming that the ballast stiffness directly influences the natural frequencies of the system. Additionally, higher stiffness reduces receptance across the frequency spectrum, confirming reduced strain under dynamic loading.

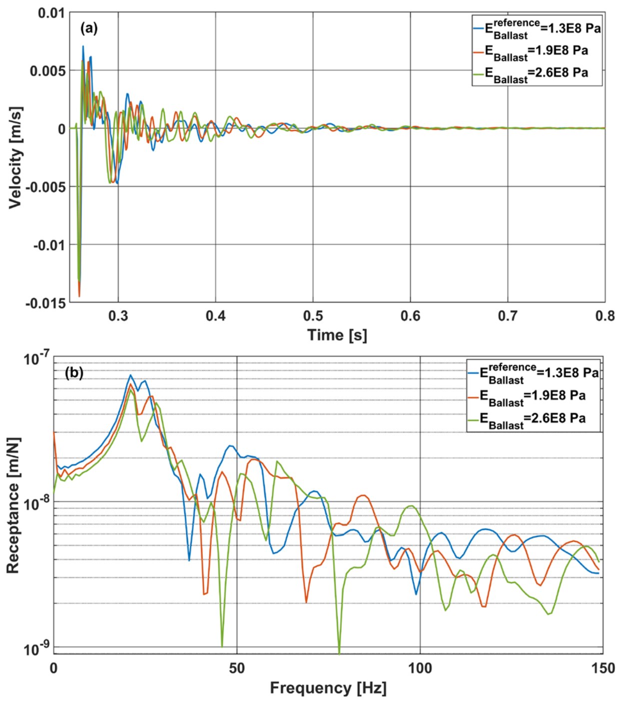

Fig. 9. Influence of ballast stiffness on the ballast vibration in terms of (a) time domain and (b) frequency domain.

4.4.2 Ballast layer damping

Increasing the ballast layer damping results in a reduction in vibration amplitudes throughout the entire time history (Fig. 10a), reflecting enhanced energy dissipation within the ballast layer. Higher damping also leads to faster attenuation of vibrations and shorter stabilisation times following excitation. While the low frequency response remains largely unaffected by variations in damping, significant differences are observed at higher frequencies. In cases with lower ballast damping, larger vibration amplitudes and more pronounced oscillatory behaviour are evident, indicating that high frequency components are insufficiently attenuated. In contrast, increased damping effectively suppresses these components, resulting in a smoother and more rapidly decaying time domain response.

In the frequency domain (Fig. 10b), the first resonance peak remains unaffected by variations in ballast damping, whereas reductions are observed for frequency modes above 25 Hz. Increasing ballast damping results in a smoother FRF response, with a reduction in the amplitude and sharpness of higher order peaks. The results show the dominant role of ballast damping in controlling system response above 25 Hz.

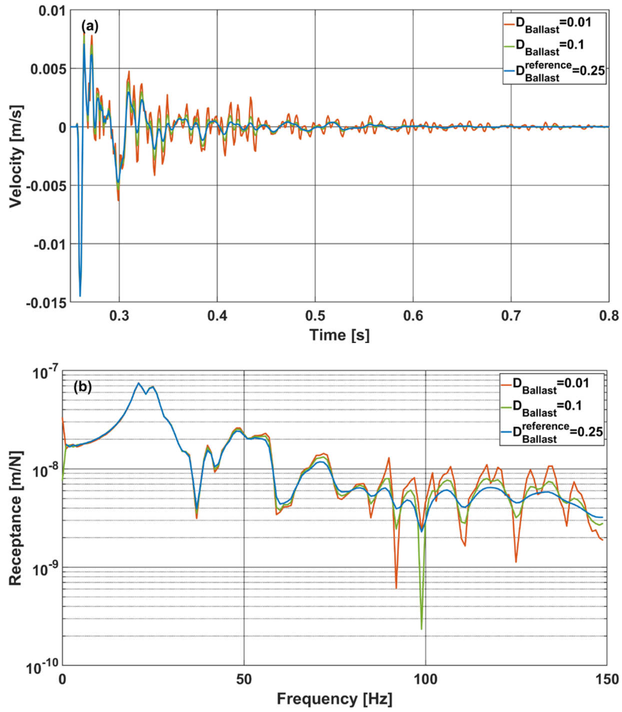

Fig. 10. Influence of ballast damping on the ballast vibration in terms of (a) time domain and (b) frequency domain.

4.5 Influence of base (foundation) properties

Increasing the stiffness of the base springs reduces vibration amplitudes across the entire time history, including both initial peak and subsequent oscillations (Fig. 11a), because of improved overall support conditions and reduced deformation at the foundation level. Higher base stiffness results in faster vibration attenuation, reflecting increased system constraint and reduced energy storage in the lower boundary.

In the frequency domain (Fig. 11b), increasing base stiffness shifts the first and second resonance frequencies toward higher values, while higher frequency modes remain unaffected. For sufficiently high stiffness values, the system behaves as a rigidly supported structure, and low frequency modes shift significantly upward beyond 100 Hz, indicating strong coupling between foundation stiffness and global system dynamics.

Increasing base damping also reduces vibration amplitudes throughout the entire time history (Fig. 12a) and accelerates vibration decay, resulting in faster stabilisation after impact excitation. In the frequency domain (Fig. 12b), base damping does not significantly alter natural frequencies. However, it leads to a substantial reduction in FRF amplitude, particularly in the frequency range up to 80 Hz where global track-foundation modes dominate. Increasing damping above its critical value smoothens the FRF response at the lower frequencies and reduces dynamic amplification over the entire frequency range.

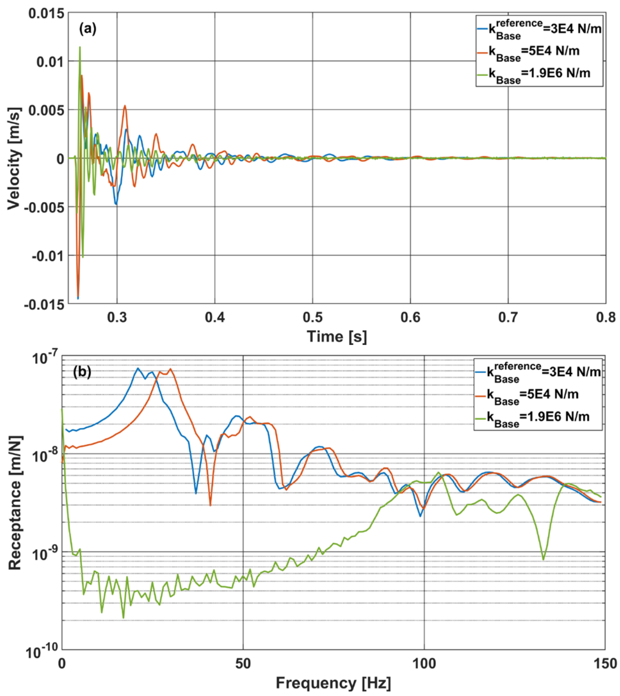

Fig. 11. Influence of base stiffness on the ballast vibration in terms of (a) time domain and (b) frequency domain.

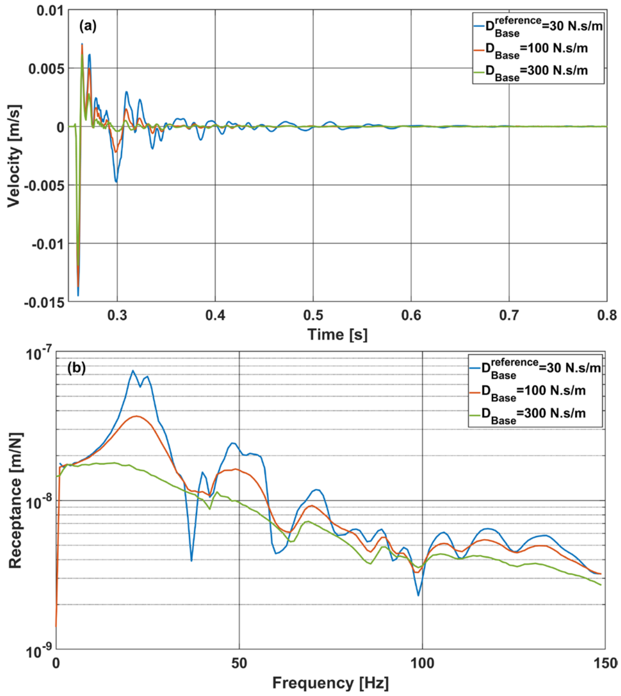

Fig. 12. Influence of base damping on the ballast vibration in terms of (a) time domain and (b) frequency domain.

5 Conclusions

This study focused on the development of a finite element modelling framework for simulating the dynamic response of a railway track superstructure subjected to hammer impact. A 3D FE model of the rail-sleeper-ballast system was developed in LS-DYNA, to investigate the influence of key track component properties on the system response and identify those components that dominate the propagation in the subsoil. Laboratory hammer impact test results, coming from a previous investigation in the laboratory, were used to assist the development of the model.

The model parameters were selected based on representative values reported in the literature. Detailed parameter calibration was not performed at this stage. The comparison between numerical results and experimental data indicated reasonable agreement in both time and frequency domains, showing that the model can capture the essential dynamic characteristics of the track-ballast system within the investigated frequency range. A parametric analysis was conducted to evaluate the sensitivity of the system response to variations in the selected model parameters within a reasonable range.

The parametric analysis provided an insight into the role of individual track components in governing vibration transmission:

- Fastener properties primarily influence above 80 Hz frequency response of the system, while they hardly affect the dominant lower frequencies modal vibration.
- Ballast properties influence the vibration modes and energy dissipation in the frequency interval from 25 Hz to around 60 Hz. Increasing ballast stiffness shifts resonance frequencies to higher values, whereas increased ballast damping significantly reduces vibration amplitudes, particularly at higher frequencies, and leads to a smoother frequency response.
- The base (foundation) properties govern the first mode of vibration of the system (20-25 Hz). Increasing base stiffness shifts the fundamental natural frequency, while base damping reduces overall vibration amplitudes, especially in the lower frequency range of the system response.

The identification of the frequency dependent behaviour of the track system reveals that different components govern distinct frequency ranges. Higher frequency vibrations are mainly associated with the upper track components (rail and fastener), whereas lower frequency response is governed by the ballast and underlying support conditions. The dominant mode (20-25 Hz) is well caught, given that the parameters were not specifically calibrated. However, in the range between 30 Hz and 70 Hz, the resonance behaviour resulting from the numerical analysis does not match the measured response accurately. This range of frequencies is governed mostly by the ballast-sleeper system, and the difference between experimental data and numerical results suggests that a more refined strategy is needed in the future to better decouple the two elements. Previous studies [17] have shown that the introduction of interface elements at the sleeper-ballast and ballast-subsoil interfaces can improve the representation of contact behaviour and load transfer mechanisms, leading to a more accurate prediction of the dynamic response of the track system.

In the field, the rail-sleeper-ballast system functions as a frequency-selective filter, progressively attenuating high-frequency vibration energy, while allowing lower-frequency components to propagate into the foundation and subsoil layers. Recent field measurements on railway tracks founded on soft soils have shown that the first dominant natural frequency associated with the coupled embankment-subsoil system typically occurs within the range of 20-30 Hz [18]. A comparable low-frequency response is also observed in the present FE analyses when relatively soft base stiffness values are introduced, mimicking soft clays and peats subsoil conditions. Accurate calibration of the foundation stiffness and damping is therefore essential to predict the vibration propagation in the ground and assess the long-term performance of the railway infrastructure on soft soils.

The authors acknowledge the financial support of ProRail, NL, through the research programmes RESET and STEM.

References

1. H.-Y. Zhao, B. Indraratna, and T. Ngo, Numerical simulation of the effect of moving loads on saturated subgrade soil, Comput. Geotech., vol. **131**, p. 103930, (Mar. 2021), doi: 10.1016/j.compgeo.2020.103930.
2. B. Indraratna and W. Salim, Mechanics of ballasted rail tracks: a geotechnical perspective. CRC Press, (2005).
3. W. Powrie, L. Le Pen, D. Milne, and D. Thompson, Train loading effects in railway geotechnical engineering: Ground response, analysis, measurement and interpretation, Trans. Geotech., vol. **21**, p. 100261, (Dec. 2019), doi: 10.1016/j.trgeo.2019.100261.
4. J. Liu and J. Xiao, Experimental Study on the Stability of Railroad Silt Subgrade with Increasing Train Speed, J. Geotech. Geoenviron. Eng., vol. **136**, no. 6, pp. 833–841, (Jun. 2010). doi: 10.1061/(ASCE)GT.1943-5606.0000282
5. L. Wang, P. Wang, K. Wei, R. Dollevoet, and Z. Li, Ground vibration induced by high speed trains on an embankment with pile-board foundation: Modelling and validation with in situ tests, Trans. Geotech, vol. **34**, p. 100734,(May 2022). doi: 10.1016/J.TRGEO.2022.100734
6. S. Atapattu, B. Indraratna, and C. Rujikiatkamjorn, Influence of periodic cyclic loading and rest period on soft clay consolidation, Proceedings of the Institution of Civil Engineers - Ground Improvement, vol. **177**, no. 1, pp. 30–43, (Mar. 2024), doi: 10.1680/jgrim.22.00082.
7. M. Naeimi, Z. Li, R. H. Petrov, J. Sietsma, and R. Dollevoet, Development of a New Downscale Setup for Wheel-Rail Contact Experiments under Impact Loading Conditions, Exp. Tech. 2017 42:1, vol. **42**, no. 1, pp. 1–17, (Oct. 2017), doi: 10.1007/S40799-017-0216-Z.
8. C. Cengiz, T. Schweckendiek, A. van Uitert, and C. Zwanenburg, Centrifuge modelling of railway embankments on soft clay: load-displacement behaviour, pore pressure development, and deformation mechanisms, Trans. Geotech., under review, (2026).
9. B. Feng et al., Advanced full-scale laboratory dynamic load testing of a ballasted high-speed railway track, Trans. Geotech, vol. **29**, p. 100559, (Jul. 2021), doi: 10.1016/j.trgeo.2021.100559.
10. A. Al Shaer, D. Duhamel, K. Sab, G. Foret, and L. Schmitt, Experimental settlement and dynamic behavior of a portion of ballasted railway track under high speed trains, J. Sound Vib., vol. **316**, no. 1–5, pp. 211–233, (Sep. 2008).
11. Ansys, ANSYS LS-DYNA KEYWORD USER'S MANUAL VOLUME I LS-DYNA Dev ANSYS PART OF SYNOPSYS, (2026) Available: http://www.ansys.com
12. X. Yuan, S. Zhu, and W. Zhai, Dynamic performance evaluation of rail fastening system based on a refined vehicle-track coupled dynamics model, Veh. Syst. Dyn., vol. **60**, no. 8, pp. 2564–2586, (Aug. 2022). doi: 10.1080/00423114.2021.1913193.
13. W. Powrie, Railway track substructure: Recent research and future directions, Trans. Geotech., vol. **46**, p. 101234, (May 2024). doi: 10.1016/J.TRGEO.2024.101234.
14. C. Ngamkhanong, Q. Y. Ming, T. Li, and S. Kaewunruen, Dynamic train-track interactions over railway track stiffness transition zones using baseplate fastening systems, Eng. Fail. Anal., vol. **118**, p. 104866, (Dec. 2020). doi: 10.1016/J.ENGFAILANAL.2020.104866.
15. G. Kouroussis, L. Van Parys, C. Conti, and O. Verlinden, Using three-dimensional finite element analysis in time domain to model railway-induced ground vibrations, Advances in Engineering Software, vol. **70**, pp. 63–76, (Apr. 2014). doi: 10.1016/J.ADVENGSOFT.2014.01.005.
16. Ansys, LS-DYNA Theory Manual LS-DYNA Dev ANSYS, (1992), Available: https://lsdyna.ansys.com
17. J. Xiao, L. Xue, D. Zhang, S. Sun, Y. Bai, and J. Shi, Coupled DEM-FEM methods for analyzing contact stress between railway ballast and subgrade considering real particle shape characteristic, Comput. Geotech., vol. **155**, p. 105192, (Mar. 2023) doi: 10.1016/J.COMPGEO.2022.105192.
18. S. Gong, L. Wang, C. Shen, C. Jommi, and Z. Li, Resonance behaviour of railway embankments on soft subsoil, (2026), This volume.